CrossMark

Bone Strength in Growing Rats Treated with Fluoride: a Multi-dose Histomorphometric, Biomechanical and Densitometric Study

Brenda Lorena Fina [1,2] · Maela Lupo [1,2,3] · Eugenia Rocío Da Ros [1] · Mercedes Lombarte [1,2,3] · Alfredo Rigalli [1,2,3]

Abstract

Bone deformation and fragility are common signs of skeletal fluorosis. Disorganisation of bone tissue and presence of inflammatory foci were observed after fluoride (F^-) administration. Most information about F^- effects on bone has been obtained in adult individuals. However, in fluorosis areas, children are a population very exposed to F^- and prone to develop not only dental but also skeletal fluoroses. The aim of this work was to evaluate the bone parameters responsible for the effect of different doses of F^- on fracture load of the trabecular and cortical bones using multivariate analysis in growing rats. Twenty-four 21-day-old Sprague-Dawley rats were divided into four groups: F0, F20, F40 and F80, which received orally 0, 20, 40 or 80 μmol F^-/100 g bw/day, respectively, for 30 days. After treatment, tibiae were used for measuring bone histomorphometric and connectivity parameters, bone mineral density (BMD) and bone cortical parameters. The femurs were used for biomechanical tests and bone F^- content. Trabecular bone volume was significantly decreased by F^-. Consistently, we observed a significant decrease in fracture load and Young's modulus (YM) of the trabecular bone in F^--treated groups. However, cortical bone parameters were not significantly affected by F^-. Moreover, there were no significant differences in cortical nor trabecular BMD. Multivariate analysis revealed a significant correlation between the trabecular fracture load and YM but not with bone volume or BMD. It is concluded that when F^- is administered as a single daily dose, it produces significant decrease in trabecular bone strength by changing the elasticity of the trabecular bone.

Introduction

Fluorine in its elemental form (F_2) is a gaseous compound but, because of its high electronegativity, in nature, it is found only as fluoride (F^-). It is one of the 20 most abundant elements in the earth's crust and is part of minerals such as fluorite (CaF_2), fluorapatite ($Ca_5(PO_4)_3F$) and cryolite (Na_3AlF_6) [1]. Fluorine content is high in some foods, such as fish, tea [2] and vegetables grown on areas with high fluorine content in soils [3, 4].

However, the most common form of F^- uptake is the drinking water.

F^- is a trace element with opposite effects on human beings. There are different reports about the beneficial or deleterious effects that F^- has on bones and consequently how it compromises the mechanical behaviour of the bone as a supporting structure. On one hand, its daily administration prevents teeth caries and has a mitogenic action on osteoblasts [5], but on the other hand, in areas where concentrations of F^- in water exceed the limit recommended by the World Health Organization (WHO) (1.5 ppm), dental fluorosis could be seen [6]. Although WHO established 1.5 ppm, dental fluorosis could appear with lower concentration of F^- in drinking water as a consequence of increasing intake from other sources [7]. Skeletal fluorosis appears after high F^- content (over 3 ppm) is consumed and is clinically characterized by alterations in teeth, musculo-skeletal, endocrine and nervous systems [8]. When drinking water contains over 10 ppm of F^-, more serious effects on skeletal tissue could be seen and crippling fluorosis could be developed [9].

✉ Brenda Lorena Fina
brendafina@conicet.gov.ar

1   Bone Biology Laboratory, School of Medicine, Rosario National University, Rosario S2002KTR, Santa Fe, Argentina

2   National Council of Scientific and Technical Research (CONICET), Buenos Aires, Argentina

3   Rosario National University Research Council, Rosario, Argentina

🍁 Springer

F^- is mainly incorporated into the bone during bone formation and removed by bone resorption. F^- replaces the hydroxyl group in hydroxyapatite crystal transforming it into fluorapatite [10], more stable and less soluble in acidic solutions than hydroxyapatite [11]. The proportion of F^- that is incorporated by bone tissue depends on the amount ingested, time and type of exposure, age, tissue metabolism [1] and genetic factors [12].

The increase in bone mass and bone growth takes place in childhood [13, 14], so that growing people are the most affected by high F^- intake because this ion has high affinity for bone tissue and children's bones have a higher rate of modelling than adults' bones. Children living in fluorosis areas could manifest not only dental but also skeletal fluorosis with severe bone deformities [15, 16]. Children are a special population who are exposed to F^- not only by the consumption of fluoridated water but also from the ingestion of F^- from toothpaste and varnishes: 81.5% of the average daily intake of F^- comes from these products [17, 18]. Biomechanical bone properties depend on nano-parameters such as the structure of collagen type I, osteocytes network and hydroxyapatite crystals. Bone fractures are determined not only by bone mass, but also by bone tissue quality such as collagen and mineral properties [19]. F^-'s treatment decreased nitric oxide response to mechanical loading and affected the arrangement and amount of F-actin in MC3T3-E1 osteoblasts. Also, F^- treatment resulted in more elongated and smaller osteocytes in hamster mandibles in vivo [20]. Previous studies done in our laboratory revealed that the disorganisation of bone tissue [21] and the presence of inflammatory foci [22] when sodium fluoride (NaF) is administered could be the cause of bone alterations. Subsequent studies showed that inflammation at bone level is due to an increased release of superoxide that determines the increase in reactive oxygen species and tissue damage [23].

There are many studies that showed the effects of F^- on the bone. However, the cause of the negative effects of F^- on the bone has not been explained yet. It is known that F^- in high concentrations increases bone fragility in adult individuals, but it has not been studied whether this increase is due to loss of bone mass, elasticity, mineral density or trabecular connectivity. To know the first changes on the bone in fluorosis, it is necessary to study the effects that occur from the beginning in the fluoride consumption. Therefore, variables that determine bone fragility in fluoride exposure of a growing child are still unknown. The aim of this work was to evaluate the effect of different F^- doses on biomechanical and morphometric properties of the trabecular and cortical bones by a multivariate analysis to identify which of those variables determine the fracture load in growing rats.

Materials and Methods

Animals and Study Design

Experiments were carried out on 21-day-old female Sprague-Dawley rats (body weight 78.4 ± 12.8 g). The rats were housed in collective cages with water and balanced food ad libitum (Gepsa, Pilar, Córdoba, Argentina). During the experiments, the rats were kept in a temperature-controlled environment of 23–25 °C, with a 12-h light:12-h darkness cycle and filtered airflow at scheduled time intervals. The animals were treated according to the accepted international standards for animal care [24, 25], and the study has been approved by the Ethical Committee of the School of Medicine of Rosario National University.

The rats were randomly divided into four groups ($n = 6$/group): F0, F20, F40 and F80, which received orally, through a gastric catheter, 0, 20, 40 or 80 μmol F^-/100 g bw/day (equivalent to 0, 0.4, 0.8 and 1.6 mg F^-/100 g/day), respectively, for 30 days. F^- was administered as sodium fluoride (Sigma-Aldrich, USA).

The doses of F^- administered are comparable to those used in several previous works to study the toxic effects of F^- in rats [26–28]. Treatment was carried out from weaning (day 21) to reproductive maturation of the rat (day 53), in order to study the effect of F^- during childhood and bone modelling.

After treatment, body weight was evaluated, euthanasia by CO_2 inhalation was performed and tibiae and femurs were extracted. Blood samples were collected by heart puncture into heparinized tubes, which were centrifuged at $1400 \times g$ and cut at the buffy coat level. Urine was recollected in individual metabolic cages for 24 h before euthanasia. Plasma and urine were used for F^- measurement.

Histomorphometric and connectivity parameters, bone mineral density (BMD) and cortical parameters were evaluated in the tibiae. Both femurs were used for F^- content measurements and biomechanical tests to evaluate trabecular and cortical bone resistance.

Bone Histomorphometry

After euthanasia, the proximal epiphysis of the left tibia was fixed in 10% phosphate-buffered formaldehyde, decalcified in 10% EDTA, dehydrated through ascending ethanol concentrations and embedded in paraffin. Longitudinal 5-μm-thick sections of proximal tibia metaphysis was obtained with a microtome (Mikoba 320, China) and stained with hematoxylin-eosin. Permanent slides were examined using a light microscope (Leitz, Wetzlar, Germany). Digital images of trabecular bone were obtained at a $\times 40$ magnification with a camera (Olympus SP-350, China). A 2-mm^2 region of interest (ROI) at 1-mm distal from the growth plate-metaphyseal junction was selected. This ROI was considered the total tissue volume. ROIs were analysed with ImageJ 1.40 (National

Institutes of Health, Maryland, USA). As described by Parfitt et al. [29], the following measurements were performed: (1) total tissue volume (TV, μm^2) and (2) trabecular bone volume (BV, μm^2). With these values, bone volume (BV/TV, %) was calculated as BV $\times$ 100/TV.

Trabecular Connectivity Assessment

The analysis of trabecular interconnectivity was performed as previously published [30, 31]. The following parameters were measured on the 5-μm-thick sections of proximal tibia metaphysis stained with hematoxylin-eosin using ImageJ 1.40 software: total number of nodes (Nd) and number of terminals (Tm). With these parameters, we proceeded to calculate an interconnectivity parameter known as node-to-termini ratio ($R =$ Nd/Tm). The greater the value of R, the more connectivity the trabecular bone has.

Morphometric Analysis of the Cortical Bone

Cross-sections (1-mm thick) of the diaphysis of the right tibiae were cut with a low-speed saw (IsoMet, Buehler Ltd., IL, USA) at 50% of the total length. A digital image was obtained at $\times$ 40 magnification with a digital camera (Olympus SP-350, China), and measurements were performed with ImageJ 1.40 software [32]: (1) cross-sectional area, the area of bone and marrow cavity bounded by the periosteal surface (mm^2), and (2) medullary area, the area delineated by the endocortical surface (mm^2). With these values, cortical bone area (CA) was calculated as the difference between the cross-sectional area and the medullary area (mm^2). The CA indicates the volume of the cortical bone.

Bone Mineral Density

BMD (mg Ca^{2+}/cm^2) in the right tibia was measured by X-ray absorptiometry (Work Ray, Buenos Aires, Argentina, 70KV, 8 mA) [33]. Measurements were done on digital images with ImageJ 1.40 software. For measurement of BMD, the total area of the tibia was delimited to calculate the total BMD. Then, the midpoint of its length was marked and an area of 0.7 mm^2 was delimited in order to measure the cortical BMD (cBMD) in the same place where cortical morphometric measurements were performed. Finally, an area of 2 mm^2 at 1-mm distal from the growth plate-metaphyseal junction was delimited to measure trabecular BMD (tBMD) in the same area where histomorphometric and connectivity measurements were performed.

Mechanical Testing

Both femurs were extracted after euthanasia, stored at $-20\ ^\circ C$, wrapped in saline-soaked gauze until tested and then thawed at 37 $^\circ C$. The cortical bone strength at midshaft of both femurs was determined with a three-point bending test, and femurs were bent about the anterior-posterior axis [34]. The trabecular bone strength was determined by a compression test in distal epiphysis of both femurs as detailed below [35]. The mechanical test was performed on a mechanical testing machine designed in the engineering department of the Bone Biology Laboratory, with a 300-N load cell with 0.01 N of discrimination and an accuracy of 10 μm in displacements. The support span in the three-point bending test was 11 mm. The area of the circular compression platen was 7.07 mm^2, and a 2.5-mm-thick transversal section of distal epiphysis of femurs was used. For both tests, the speed was 0.01 mm/s and was monitored on a computer. Load-versus-displacement plots were recorded using the software Biomedical Data Acquisition Suite 1.0 (Argentina, 2011) to determine bone properties. The software data acquisition rate was 10 Hz. The fracture load (Fx, N) was recorded as the load the bone fractured, and stiffness (N/mm) was determined as the slope of the linear portion of the load-versus-displacement curve. The cross-sectional moment of inertia (CSMI, mm^4) was determined in a 1.5-mm-thick transversal section obtained by a low-speed diamond saw, and the outer (od) and inner diameters (id) were obtained in digital images using the ImageJ 1.40 software. CSMI was calculated as $\pi(od^4 - id^4)/64$. The material properties were determined by employing classic beam theory and transforming the data of load and displacement in stress [stress = load $\times$ support span $\times$ outer radius/(4 $\times$ CSMI)] and strain [strain = (12 $\times$ outer radius $\times$ displacement $\times 10^6$)/(support span)^2], respectively. The modulus of elasticity or Young's modulus (YM, GPa) was calculated using the linear portion of the stress versus strain curve and indicates tissue elasticity.

Fluoride Measurements

Serum and bone levels were measured by direct potentiometry using an ion-selective electrode, ORION 94-09, Orion Research (MA, USA), after isothermal distillation [36]. Prior to measurements, bone tissue was incinerated for 6 h at 550 $^\circ C$. Urine F^- was measured by direct potentiometry using the same electrode explained before.

Statistical Analysis

Data are expressed as mean $\pm$ SEM. Statistical analyses were performed with R 2.14.1 software [37]. One-way ANOVA was used for group comparisons. Differences were considered significant when $p < 0.05$, and LSD post-test was used. The statistical power was calculated for the comparisons when significant differences were observed. One-way ANOVA power test was used for the calculation, and pwr library was used. To assess which bone parameter explains the fracture load, linear model analysis was used (lm package in R software).

Results

The body weights of the animals at the beginning of the experiment were not different between groups: F0, 86 ± 39 g; F20, 75 ± 35 g; F40, 74 ± 21 g; F80, 78 ± 36 g. After treatment, final body weight was not affected by F^-: F0, 233 ± 38 g; F20, 228 ± 44 g; F40, 226 ± 35 g; F80, 207 ± 41 g (one-way ANOVA, $p > 0.05$).

Although a decrease in serum fluoride was observed in all F^--treated groups, this difference was only statistically significant for the F40 group (Table 1). In turn, a significant increase in urine fluoride was observed as the doses of F^- increased. As expected, bone F^- content increased significantly with F^- doses. This result would ensure that the treatments with F^- had their action in the bone, producing a stimulus of the bone tissue and an increase in the incorporation of F^-.

Effects of F^- on the Trabecular Bone

A significant decrease in the trabecular fracture load was observed in F^--treated rats, independently of F^- dose (Table 2), and a significant decrease in trabecular stiffness in F40 and F80 compared to F0 was also observed. Furthermore, a significant decrease in trabecular bone volume, Young's modulus and the connectivity index R was observed in F40 and F80 groups compared to F0 group, without changes in trabecular bone mineral density.

Illustratively, Fig. 1 shows representative histological sections of the tibia of one rat from each experimental group. The loss of trabecular connectivity and bone mass as the dose of F^- increased can be observed. The bone slices show visibly different effects of F^- on bone structure.

Determination of Variables Affecting Trabecular Resistance

The variables that affected trabecular bone resistance were analysed by employing linear modelling. tFx was considered as dependent variable, and tYM, BV/TV, tBMD, bone F^- content (F) and R were the independent variables. Therefore, we analysed the following linear model:

$$\mathrm{tFx} = a^*\mathrm{tYM} + b^*\mathrm{BV/TV} + c^*R + d^*\mathrm{tBMD} + e^*F + f$$

where a, b, c, d, e and f are the coefficients of the model.

Linear model analysis revealed that trabecular fracture load depended significantly on Young's modulus (estimate coefficient 193 ± 63, $p < 0.05$) and did not depend on any other parameter analysed ($R^2 = 0.56$, adjusted $R^2 = 0.42$, $p = 0.013$, power 0.97).

Therefore, linear model analysis was done again considering only Young's modulus, and the model for trabecular fracture load in F^--treated rats was

$$\mathrm{tFx} = 198^*\mathrm{tYM} + 14.3$$

with an $R^2 = 0.57$ and an adjusted $R^2 = 0.56$; $p = 5.9 \times 10^{-9}$.

Figure 2 showed that the higher the dose of F^- used, the lower the fracture load and the Young's modulus. In conclusion, F^--induced decrease in trabecular bone resistance is explained largely by tissue elasticity.

Effects of F^- on the Cortical Bone

There were no effects of F^- on fracture load (cFx), Young's modulus (cYM), CA and cBMD at the level of the midshaft of the femur. However, a significant decrease in the stiffness and the CSMI was only observed in the F80 group compared to F0 (Table 3).

The linear model analysis was not performed for the cortical bone because fracture load was not affected by F^-.

Discussion

F^- has been used for many years for the treatment of bone diseases such as osteoporosis, since it was observed to increase bone mineral density and reduce pain [38]. However, F^- has been shifted from the pharmaceutical market because it produced an increased risk of fractures and due to the discovery of other drugs (bisphosphonates, monoclonal antibodies) with better efficacy on the bone [39]. In addition, F^- is still

Table 1 Serum (μmol/l), urine (μmol F^-/24 h) and bone (mg F^-/g ashes) fluoride of groups treated with 0, 20, 40 or 80 μmol F^-/100 g bw/day

	F0	F20	F40	F80	Power
Serum fluoride	183.5 ± 70.8^a	102.0 ± 93.3^{ab}	65.7 ± 62.2^b	93.9 ± 79.5^{ab}	0.55
Urine fluoride	1.86 ± 1.30^a	6.46 ± 2.13^{ab}	6.94 ± 3.15^c	13.15 ± 7.75^d	0.98
Bone fluoride	0.62 ± 0.23^a	2.88 ± 0.35^b	7.22 ± 0.24^c	8.15 ± 0.54^c	1

Data are shown as means ± SEM. At least one similar superscript letter between two cells of the same row indicates no significant differences between group means. The last column shows the statistical power of each comparison. One-way ANOVA, LSD post test, $p < 0.05$

Table 2 Trabecular parameters of bone resistance, mineral density and bone volume of experimental groups treated with 0, 20, 40 or 80 μmol F⁻/100 g bw/day

Trabecular parameters	F0	F20	F40	F80	Power
Fracture load (N)	45.1 ± 8.0[a]	24.4 ± 2.8[b]	25.1 ± 4.2[b]	16.7 ± 2.6[b]	0.90
Stiffness (N/mm)	331 ± 99[a]	170 ± 45[ab]	148 ± 41[b]	125 ± 35[b]	0.52
Bone volume (%)	22.1 ± 1.4[a]	21.2 ± 1.4[ab]	18.2 ± 0.9[bc]	15.8 ± 1.6[c]	0.75
Young's modulus (GPa)	0.12 ± 0.04[a]	0.06 ± 0.02[ab]	0.05 ± 0.01[b]	0.04 ± 0.01[b]	0.61
Node-to-termini parameter	0.34 ± 0.04[a]	0.39 ± 0.02[a]	0.23 ± 0.02[b]	0.17 ± 0.04[b]	0.99
Bone mineral density (mg Ca/cm²)	27.2 ± 3.2[a]	25.8 ± 4.3[a]	27.2 ± 3.1[a]	22.2 ± 1.5[a]	–

Data are shown as means ± SEM. At least one similar superscript letter between two cells of the same row indicates no significant differences between group means. The last column shows the statistical power of each comparison. One-way ANOVA, LSD post test, $p < 0.05$

used for topical therapies in the teeth and many countries added it to drinking water. However, lots of countries have natural F⁻ in their well water. China, India and Tanzania are the countries most affected by the high amount of F⁻ in the water and by the number of people who consume it [40, 41]. In Argentina, we found high concentrations of F⁻ in drinking water in Buenos Aires [42], southwest of Santa Fe [43, 44], and Chaco [45] provinces. F⁻ uptake higher than 3 ppm in drinking water can lead to skeletal fluorosis, the main effect of which is bone fragility. Children in areas of fluorosis are a population with a high probability of developing skeletal fluorosis with bone deformations and bone fragility.

The primary function of the bone is to provide structural support for the body. Regarding this function, the skeleton is the basis of posture, locomotion, daily load resistance and protection of internal organs. Tissue quality depends on many factors such as the amount, connectivity and orientation of the trabeculae; the structure of collagen; mineral content and mineral density [46]. The findings of this study indicate that the loss of bone strength by F⁻ is explained by factors other than only bone mineral density.

The causes of bone fragility in skeletal fluorosis are not yet well-known. Therefore, in this study, we evaluated which bone parameters are affected by F⁻ leading to a decrease in bone strength. To study the initial changes in bone tissue of skeletal fluorosis, that is from the beginning of fluoride consumption in early ages, growing rats were used and the treatment was applied throughout the youth of the rats.

Serum F⁻ in the animals decreased and urine F⁻ increased as the administered F⁻ doses increased. These results were accompanied by a progressive increase in bone F⁻ content. Previous studies have shown that administration of a dose of

Fig 1 Micrographs showing trabecular bone sections of rat tibiae from all experimental groups. H&E × 40. In order to simplify interpretation, the bone trabeculae are outlined
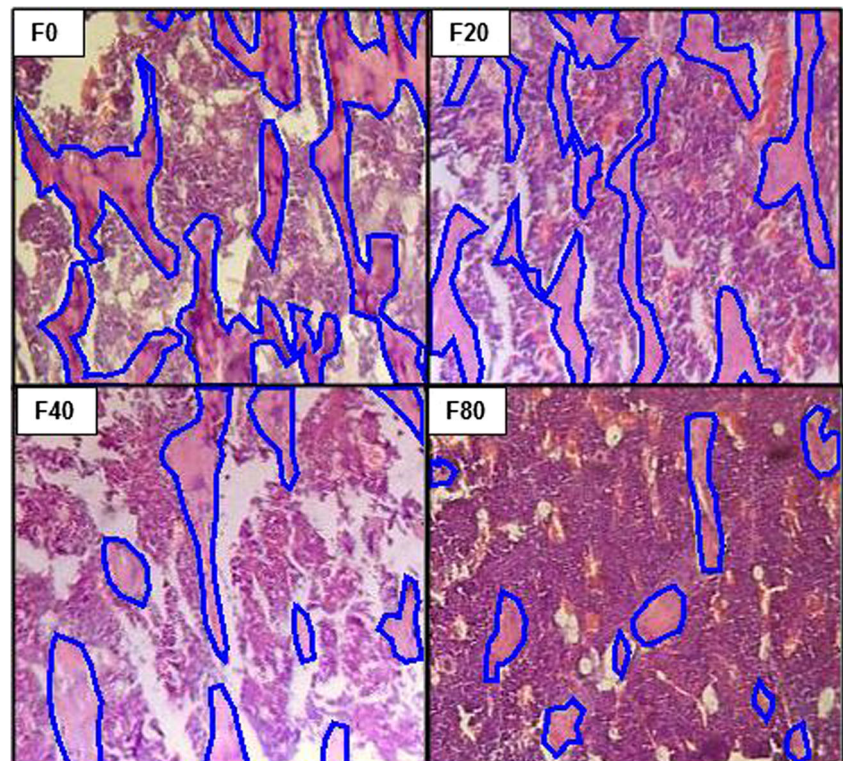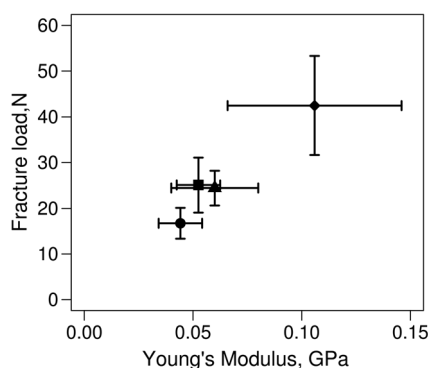
Fig 2 Fracture load (tFx, N) versus Young's modulus (GPa) of the trabecular bone of experimental groups. Points indicate the mean of each group, and segments indicate the SEM. Treatments: diamond: F0, triangle: F20, square: F40, circle: F80

40 μmol/100 g pc of NaF generated serum fluoride levels of up to 130 μmol/l and that the higher the F^- content in the bone, the less the serum F^- [47, 48] and that the higher the F^- dose, the higher the urine F^- [49, 50]. These studies suggest that F^- in high doses generates a bony stimulus that produces a greater incorporation of F^- in the tissue by which the serum F^- decreases.

Anyway, there are many authors who describe an increase in serum F^- with high doses of it administered [51, 52]. The difference found in such works could be due to various reasons: the age of the rats, their sex or the form of F^- administration (orogastric tube or drinking water). Nevertheless, as has been previously described, the severity of the expression of fluorosis depends also on the genetic background of the animals [8]. A previous work demonstrated that different strains of mice developed resistance or susceptibility to dental fluorosis with high doses of F^- [53]. In our study, Sprague-Dawley rats were used but other researchers used Wistar rats. Therefore, the discrepancies in bone responses to F^- and, therefore, in fluoremia could be due largely to the strain of rat used.

Although the dose of F80 group is twice that of F40 group, this did not generate a much greater incorporation of F^- in the bone or a much lower serum F^-; besides, a greater damage in the bone parameters was observed. Previous work has shown

that at doses greater than 100 μmol/day of F^-, there was inhibition of intestinal absorption of F^- in rats, which caused serum and bone F^- to be similar to doses a little lower than this [26].

At trabecular level, all doses of F^- significantly decreased bone strength, as measured by tFx, accompanied by a decrease in trabecular bone volume, Young's modulus, connectivity and stiffness without changes in bone mineral density. To determine which of these parameters affected tFx the most, a linear model analysis was used, which determined that the decrease in trabecular resistance by F^- is explained largely by variations in Young's modulus. Young's modulus is a measure of bone elasticity and indicates trabecular tissue quality. This parameter includes reordering of the trabeculae, its connectivity and collagen and non-collagen protein syntheses [54]. We also observed that F^- affected the connectivity parameter of the trabecular bone, so YM could be reduced because of the decrease on R values as a function of F^- doses. The results found in this work are consistent as connectivity and realignment of the trabeculae act as an elastic mesh resistant to external forces. That is, the amount of cancellous bone is not so important but how it is spatially arranged.

At the cortical level, the maximum dose of F^- decreased the stiffness and moment of inertia, but there were no changes in cFx nor in cYM.

The results found in this study also explained the atypical and spontaneous stress fractures produced by F^- in osteoporosis treatments [55]. These fractures were most frequently produced in tibial metaphysis, vertebrae and femoral neck, and in the majority of the cases, their trabecular bone volume was normal [56]. Our work demonstrated that F^- decrease in trabecular fracture load was not explained by the loss in bone volume. Also, trabecular stress fractures tended to occur in the first months of treatment, and cortical stress fractures occurred after them [57]. As we could see, cortical fracture load was not affected by F^- in the time we used for the experiment, and maybe more time of treatment with F^- is required for changes to be observed.

Finally, the higher the dose of F^- used, the lower the fracture load, bone volume and Young's modulus of the trabecular

Table 3 Cortical parameters of bone resistance, mineral density and bone volume of experimental groups treated with 0, 20, 40 or 80 μmol F^-/100 g bw/day

Cortical parameter	F0	F20	F40	F80
Fracture load (N)	88.7 ± 8.8^a	81.9 ± 7.9^a	74.6 ± 5.4^a	69.2 ± 6.7^a
Stiffness (N/mm)	304 ± 38^a	261 ± 37^{ab}	230 ± 27^{ab}	178 ± 26^b
Cortical area (mm^2)	3.7 ± 0.3^a	3.6 ± 0.3^a	3.5 ± 0.2^a	3.0 ± 0.3^a
Young's modulus (GPa)	3.6 ± 0.4^a	2.8 ± 0.3^a	3.0 ± 0.4^a	2.8 ± 0.5^a
Moment of inertia	4.6 ± 0.5^a	4.9 ± 0.5^{ab}	4.5 ± 0.4^{ab}	3.5 ± 0.4^b
Bone mineral density (mg Ca/cm^2)	18.5 ± 1.5^a	17.5 ± 1.6^a	16.0 ± 1.8^a	17.4 ± 1.9^a

Data are shown as means ± SEM. At least one similar superscript letter between two cells of the same row indicates no significant differences between group means. One-way ANOVA, LSD post test, $p < 0.05$

bone. The effects of F⁻ on bone parameters are controversial. Some authors described results similar to us [58]; a weaker bony material with increased porosity in relation to increased F⁻ was found in adult humans [21, 59]. However, others demonstrated that F⁻ administration increased BMD and bone strength [60], and they found a linear correlation between those parameters [61]. Also, computational modelling of CT imaging assessed that mechanical properties of F⁻ treated bone were strongly explained by BV/TV [62]. Most of such studies were done in adult individuals although F⁻ begins to be consumed through drinking water at early ages. Therefore, our study demonstrates that the decrease in bone resistance in fluorosis illness starts with a decrease in bone elasticity of the trabecular bone.

We know that the most effective solution to avoid the development of skeletal fluorosis is to drink water without F⁻; however, in many countries, this possibility does not exist. Knowing the changes that occur early in the intake of fluoride would help to obtain a rapid diagnosis of this disease in order to be able to act before the bones become fragile or deformed, preventing those children from having a healthy life in their future.

References

1. World Health Organization (1970) Fluoride and human health. World Health Organization, Geneva
2. Cook HA (1969) Fluoride and tea. Lancet 2:329
3. Kramer L, Osis D, Wiatrowski E, Spencer H (1974) Dietary fluoride in different areas in the United States. Am J Clin Nutr 27(6):590–594
4. Fina BL, Lupo M, Dri N, Lombarte M, Rigalli A (2016) Comparison of fluoride effects on germination and growth of Zea mays, Glycine max and Sorghum vulgare. J Sci Food Agric 96(11):3679–3687. https://doi.org/10.1002/jsfa.7551
5. Caverzasio J, Palmer G, Bonjour JP (1998) Fluoride: mode of action. Bone 22:585–589
6. Gazzano E, Bergandi L, Riganti C, Aldieri E, Doublier S, Costamagna C, Bosia A, Ghigo D (2010) Fluoride effects: the two faces of Janus. Curr Med Chem 17(22):2431–2441. https://doi.org/10.2174/092986710791698503
7. Opydo-Szymaczek J, Gerreth K (2015) Developmental enamel defects of the permanent first molars and incisors and their association with dental caries in the region of Wielkopolska, Western Poland. Oral Health Prev Dent 13:461–469. https://doi.org/10.3290/j.ohpd.a33088
8. Everett ET (2011) Fluoride's effects on the formation of teeth and bones, and the influence of genetics. J Dent Res 90(5):552–560. https://doi.org/10.1177/0022034510384626
9. Moudgil A, Srivastava RN, Vasudev A, Bagga A, Gupta A (1986) Fluorosis with crippling skeletal deformities. Indian Pediatr 23(10):767–773
10. Posner AS, Eanes ED, Harper RA, Zipkin I (1963) X-ray diffraction analysis of the effect of fluoride on human bone apatite. Arch Oral Biol 8(4):549–570. https://doi.org/10.1016/0003-9969(63)90071-2
11. Grynpas MD (1990) Fluoride effects on bone crystals. J Bone Miner Res 5(S1):S169–S175. https://doi.org/10.1002/jbmr.5650051362
12. Mousny M, Omelon S, Wise L, Everett ET, Dumitriu M, Holmyard DP, Banse X, Devogelaer JP, Grynpas MD (2008) Fluoride effects on bone formation and mineralization are influence by genetics. Bone 43(6):1067–1074. https://doi.org/10.1016/j.bone.2008.07.248
13. Farr JN, Khosla S (2015) Skeletal changes through the lifespan-from growth to senescence. Nat Rev Endocrinol 11:513–521. https://doi.org/10.1038/nrendo.2015.89
14. Golden NH, Abrams SA (2014) Optimizing bone health in children and adolescents. Pediatrics 134(4):e1229–e1243. https://doi.org/10.1542/peds.2014-2173
15. Teotia M, Teotia SP, Singh KP (1998) Endemic chronic fluoride toxicity and dietary calcium deficiency interaction syndromes of metabolic bone disease and deformities in India: year 2000. Indian J Pediatr 65(3):371–381. https://doi.org/10.1007/BF02761130
16. Vilasrao GS, Kamble KM, Sabat RN (2014) Child fluorosis in Chhattisgarh, India: a community-based survey. Indian Pediatr 51(11):903–905. https://doi.org/10.1007/s13312-014-0525-6
17. De Almeida BS, Da Silva Cardoso VE, Buzalaf MAR (2007) Fluoride ingestion from toothpaste and diet in 1- to 3-year-old Brazilian children. Community Dent Oral Epidemiol 35(1):53–63. https://doi.org/10.1111/j.1600-0528.2007.00328.x
18. García-Camba de la Muela JM, García-hoyos F, Varela Morales M, González Sanz A (2009) Demonstration of fluoride systemic absorption secondary to toothbrusing with fluoride dentifrice in children. Rev Esp Salud Publica 83(3):415–425. https://doi.org/10.1590/S1135-57272009000300007
19. Guo XE (2008) What is nanomechanics of bone and why is it important? J Musculoskelet Neuronal Interact 8(7301):327–328. https://doi.org/10.1136/bmj.322.7301.1536
20. Willems HME, van den Heuvel EGHM, Castelein S, Buisman JK, Bronckers ALJJ, Bakker AD, Klein-Nulend J (2011) Fluoride inhibits the response of bone cells to mechanical loading. Odontology 99(2):112–118. https://doi.org/10.1007/s10266-011-0013-6
21. Stein ID, Granik G (1980) Human vertebral bone: relation of strength, porosity, and mineralization to fluoride content. Calcif Tissue Int 32(1):189–194. https://doi.org/10.1007/BF02408540
22. Brun LR, Roma SM, Pérez F, Rigalli A (2012) Inflamación en el tejido óseo de ratas inducida por fluoruro de sodio. Actual Osteol 8:19–28
23. Fina BL, Lombarte M, Rigalli JP, Rigalli A (2014) Fluoride increases superoxide production and impairs the respiratory chain in ROS 17/2.8 osteoblastic cells. PLoS One 9(6):e100768. https://doi.org/10.1371/journal.pone.0100768
24. Harriss DJ, Atkinson G (2011) Update—ethical standards in sport and exercise science research. Int J Sports Med 32(10):819–821. https://doi.org/10.1055/s-0029-1237378

25. Olfert ED, Cross BM, McWilliam A (1993) Guide to the care and use of experimental animals. Canadian C, Ottawa

26. Beinlich AD, Brun LRM, Rigalli A, Puche RC (2003) Intestinal absorption of disodium monofluorophosphate in the rat as affected by concurrent administration of calcium. Arzneimittel-forsch Drug Res 53(08):584–589. https://doi.org/10.1055/s-0031-1297153

27. Li W, Jiang B, Cao X, Xie Y, Huang T (2017) Protective effect of lycopene on fluoride-induced ameloblasts apoptosis and dental fluorosis through oxidative stress-mediated Caspase pathways. Chem Biol Interact 261:27–34. https://doi.org/10.1016/j.cbi.2016.11.021

28. Pulungan ZSA, Sofro ZM, Partadiredja G (2016) Sodium fluoride does not affect the working memory and number of pyramidal cells in rat medial prefrontal cortex. Anat Sci Int. https://doi.org/10.1007/s12565-016-0384-4

29. Dempster DW, Compston JE, Drezner MK, Glorieux FH, Kanis JA, Malluche H, Meunier PJ, Ott SM, Recker RR, Parfitt AM (2013) Standardized nomenclature, symbols, and units for bone histomorphometry: a 2012 update of the report of the ASBMR Histomorphometry Nomenclature Committee. J Bone Miner Res 28(1):2–17. https://doi.org/10.1002/jbmr.1805

30. Harrar K, Hamami L (2013) An interconnectivity index for osteoporosis assessment using X-ray images. J Med Biol Eng 33(6):569–575. https://doi.org/10.5405/jmbe.1294

31. Brun LR, Brance ML, Lombarte M, Maher MC, di Loreto VE, Rigalli A (2015) Effects of yerba mate (IIex paraguariensis) on histomorphometry, biomechanics, and densitometry on bones in the rat. Calcif Tissue Int 97(5):527–534. https://doi.org/10.1007/s00223-015-0043-0

32. Brun LR, Pera LI, Rigalli A (2010) Bone morphometry and differences in bone fluorine containing compounds in rats treated with NaF and MFP. Biomed Pharmacother 64(1):1–6. https://doi.org/10.1016/j.biopha.2008.10.009

33. Moreno H, Lombarte M, Di Loreto VE (2009) Bones and bone tissue. In: Rigalli A, Di Loreto VE (eds) Experimental surgical models in the laboratory rat. CRC Press, Taylor & Francis Group, Boca Raton, pp 229–232. https://doi.org/10.1201/9781420093278.ch43

34. Hoggarth CR, Bennett R, Daley-Yates PT (1991) The pharmacokinetics and distribution of pamidronate for a range of doses in the mouse. Calcif Tissue Int 49(6):416–420. https://doi.org/10.1007/BF02555853

35. Hogan HA, Ruhmann SP, Sampson HW (2000) The mechanical properties of cancellous bone in the proximal tibia of ovariectomized rats. J Bone Miner Res 15(2):284–292. https://doi.org/10.1359/jbmr.2000.15.2.284

36. Rigalli A, Alloatti R, Puche RC (1999) Measurement of total and diffusible serum fluoride. J Clin Lab Anal 13(4):151–157. https://doi.org/10.1002/(SICI)1098-2825

37. Development Core Team R (2011) R: a language and environment for statistical computing. R Foundation for Statistical Computing, Vienna

38. Vestergaard P, Jorgensen NR, Schwarz P, Mosekilde L (2008) Effects of treatment with fluoride on bone mineral density and fracture risk—a meta-analysis. Osteoporos Int 19(3):257–268. https://doi.org/10.1007/s00198-007-0437-6

39. Lombarte M, Brun LR, Brance ML et al (2014) Efecto diferencial del ácido zoledrónico sobre el hueso trabecular y cortical de ratas ovariectomizadas. Actual Osteol 10:238–246

40. Kaseva ME (2006) Contribution of trona (magadi) into excessive fluorosis—a case study in Maji ya Chai ward, northern Tanzania. Sci Total Environ 366(1):92–100. https://doi.org/10.1016/j.scitotenv.2005.08.049

41. Zhang L, Huang D, Yang J, Wei X, Qin J, Ou S, Zhang Z, Zou Y (2017) Probabilistic risk assessment of Chinese residents' exposure to fluoride in improved drinking water in endemic fluorosis areas. Environ Pollut 222:118–125. https://doi.org/10.1016/j.envpol.2016.12.074

42. Paoloni JD, Fiorentino CE, Sequeira ME (2003) Fluoride contamination of aquifers in the southeast subhumid pampa, Argentina. Environ Toxicol 18(5):317–320. https://doi.org/10.1002/tox.10131

43. de la Sota M, Puche R, Rigalli A, Fernández LM, Benassati S, Boland R (1997) Changes in bone mass and in glucose homeostasis in subjects with high spontaneous fluoride intake. Medicina (B Aires) 57(4):417–420

44. Lupo M, Fina BL, Aguirre MC, Armendariz M, Rigalli A (2012) Determination of water fluoride concentration and the influence of the geographic coordinate system and time. Water Air Soil Pollut 223(8):5221–5225. https://doi.org/10.1007/s11270-012-1273-7

45. Blanes PS, Buchhamer EE, Giménez MC (2011) Natural contamination with arsenic and other trace elements in groundwater of the Central-West region of Chaco, Argentina. J Environ Sci Health A Tox Hazard Subst Environ Eng 46(11):1197–1206. https://doi.org/10.1080/10934529.2011.598774

46. Seeman E (2008) Bone quality: the material and structural basis of bone strength. J Bone Miner Metab 26(1):1–8. https://doi.org/10.1007/s00774-007-0793-5

47. Rigalli A, Alloatti R, Menoyo I, Puche RC (1995) Comparative study of the effect of sodium fluoride and sodium monofluorophosphate on glucose homeostasis in the rat. Arzneimittelforschung 45(3):289–292

48. Rigalli A, Ballina JC, Puche RC (1992) Bone mass increase and glucose tolerance in rats chronically treated with sodium fluoride. Bone Miner 16(2):101–108. https://doi.org/10.1016/0169-6009(92)90880-M

49. Lou D-D, Guan Z-Z, Liu Y-J, Liu YF, Zhang KL, Pan JG, Pei JJ (2013) The influence of chronic fluorosis on mitochondrial dynamics morphology and distribution in cortical neurons of the rat brain. Arch Toxicol 87(3):449–457. https://doi.org/10.1007/s00204-012-0942-z

50. Lupo M, Afonso M, Buzalaf R, Rigalli A (2011) Effect of fluoridated water on plasma insulin levels and glucose homeostasis in rats with renal deficiency. Biol Trace Elem Res 140(2):198–207. https://doi.org/10.1007/s12011-010-8690-5

51. de Carvalho JG, de Oliveira RC, Buzalaf MAR (2006) Plasma as an indicator of bone fluoride levels in rats chronically exposed to fluoride. J Appl Oral Sci 14(4):238–241. https://doi.org/10.1590/S1678-77572006000400005

52. Lobo JGVM, Leite AL, Pereira HABS, Fernandes MS, Peres-Buzalaf C, Sumida DH, Rigalli A, Buzalaf MAR (2015) Low-level fluoride exposure increases insulin sensitivity in experimental diabetes. J Dent Res 94(7):990–997. https://doi.org/10.1177/0022034515581186

53. Everett ET, McHenry MAK, Reynolds N, Eggertsson H, Sullivan J, Kantmann C, Martinez-Mier EA, Warrick JM, Stookey GK (2002) Dental fluorosis: variability among different inbred mouse strains. J Dent Res 81(11):794–798. https://doi.org/10.1177/0810794

54. Alliston T (2014) Biological regulation of bone quality. Curr Osteoporos Rep 12(3):366–375. https://doi.org/10.1007/s11914-014-0213-4

55. Schnitzler CM, Wing JR, Mesquita JM et al (1990) Risk factors for the development of stress fractures during fluoride therapy for osteoporosis. J Bone Miner Res 5(S1):S195–S200. https://doi.org/10.1002/jbmr.5650051330

56. Orcel P, De Vernejoul MC, Prier A et al (1990) Stress fractures of the lower limbs in osteoporotic patients treated with fluoride. J Bone Miner Res 5(S1):S191–S194. https://doi.org/10.1002/jbmr.5650051392

57. Schnitzler CM, Wing JR, Gear KA, Robson HJ (1990) Bone fragility of the peripheral skeleton during fluoride therapy for osteoporosis. Clin Orthop Relat Res 261:268–275

58. de Cássia Alves Nunes R, Chiba FY, Pereira AG et al (2016) Effect of sodium fluoride on bone biomechanical and histomorphometric parameters and on insulin signaling and insulin sensitivity in ovariectomized rats. Biol Trace Elem Res 173(1):144–153. https://doi.org/10.1007/s12011-016-0642-2

59. Franke J, Runge H, Grau P, Fengler F, Wanka C, Rempel H (1976) Physical properties of fluorosis bone. Acta Orthop Scand 47(1):20–27. https://doi.org/10.3109/17453677608998967

60. Ghanizadeh G, Babaei M, Naghii MR, Mofid M, Torkaman G, Hedayati M (2014) The effect of supplementation of calcium, vitamin D, boron, and increased fluoride intake on bone mechanical properties and metabolic hormones in rat. Toxicol Ind Health 30(3):211–217. https://doi.org/10.1177/0748233712452775

61. Nakahara H (1995) The effect of sodium fluoride on bone mineral density and bone strength in ovariectomized rats. Nihon Seikeigeka Gakkai Zasshi 69(11):1182–1192

62. Sreenivasan D, Watson M, Callon K, Dray M, Das R, Grey A, Cornish J, Fernandez J (2013) Integrating micro CT indices, CT imaging and computational modelling to assess the mechanical performance of fluoride treated bone. Med Eng Phys 35(12):1793–1800. https://doi.org/10.1016/j.medengphy.2013.07.013